Synthetic and Systems Biotechnology 9 (2024) 234–241

Contents lists available at ScienceDirect

Synthetic and Systems Biotechnology

journal homepage: www.keaipublishing.com/en/journals/synthetic-and-systems-biotechnology

Original Research Article

Promoter engineering enables precise metabolic regulation towards efficient β-elemene production in *Ogataea polymorpha*

Min Ye [a,d], Jiaoqi Gao [a,b,c], Jingjing Li [a,c], Wei Yu [a,c], Fan Bai [a,c], Yongjin J. Zhou [a,b,c,*]

[a] Division of Biotechnology, Dalian Institute of Chemical Physics, Chinese Academy of Sciences, 457 Zhongshan Road, Dalian, 116023, PR China
[b] CAS Key Laboratory of Separation Science for Analytical Chemistry, Dalian Institute of Chemical Physics, Chinese Academy of Sciences, Dalian, 116023, PR China
[c] Dalian Key Laboratory of Energy Biotechnology, Dalian Institute of Chemical Physics, Chinese Academy of Sciences, Dalian, 116023, PR China
[d] University of Chinese Academy of Sciences, Beijing, 100049, PR China

ARTICLE INFO

Keywords:
Promoter library
Growth phase-dependent promoters
Promoter engineering
Precise metabolic regulation
Ogataea polymorpha

ABSTRACT

Precisely controlling gene expression is beneficial for optimizing biosynthetic pathways for improving the production. However, promoters in nonconventional yeasts such as *Ogataea polymorpha* are always limited, which results in incompatible gene modulation. Here, we expanded the promoter library in *O. polymorpha* based on transcriptional data, among which 13 constitutive promoters had the strengths ranging from 0–55% of P_{GAP}, the commonly used strong constitutive promoter, and 2 were growth phase-dependent promoters. Subsequently, 2 hybrid growth phase-dependent promoters were constructed and characterized, which had 2-fold higher activities. Finally, promoter engineering was applied to precisely regulate cellular metabolism for efficient production of β-elemene. The glyceraldehyde-3-phosphate dehydrogenase gene *GAP* was downregulated to drive more flux into pentose phosphate pathway (PPP) and then to enhance the supply of acetyl-CoA by using phosphoketolase-phosphotransacetylase (PK-PTA) pathway. Coupled with the phase-dependent expression of synthase module (*ERG20*~*LsLTC2* fusion), the highest titer of 5.24 g/L with a yield of 0.037 g/(g glucose) was achieved in strain YY150U under fed-batch fermentation in shake flasks. This work characterized and engineered a series of promoters, that can be used to fine-tune genes for constructing efficient yeast cell factories.

1. Introduction

Microbial cell factories have been regarded as an ecologically-friendly, sustainable, and effective way for production of chemicals. Efficient production of biofuels [1–3], terpenoids [4–7] and other valuable chemicals [8,9] have been achieved in model microbes, such as *Escherichia coli*, *Saccharomyces cerevisiae* and *Bacillus subtilis*. Chemicals with long and complex pathways require precise metabolic modulation, including compartmentalization [10], modular pathway engineering [11], and promoter engineering [12].

Promoter engineering is a feasible approach to balance gene expression for fine-tuning metabolic pathways [13,14]. For example, the balanced expression level of *4CL1* and *VST1* by exchanged promoters increased the titer of resveratrol by 2.6-fold [15], and fatty acid production was also significantly promoted by precisely regulating gene *PGI1* and *IDH2* [16]. In particular, it is critical to carefully select promoter for gene regulation during pathway optimization. Through evaluation of a combinatorial expression cassette library for mevalonate pathway genes, the medium-strength expression of *ERG12* was found to be beneficial for product biosynthesis in *S. cerevisiae* [17]. Randomly combination of promoters for optimizing the expression of pathway genes enabled enhanced glucose consumption [18], and increased production of patchoulol [19] and carotenoid [20] in *S. cerevisiae*. With the development of synthetic biology, a variety of promoters were characterized in model yeast *S. cerevisiae* [21–23] or other non-conventional yeast such as *Yarrowia lipolytica* [24,25], *Pichia pastoris* [26,27]. However, there are limited promoters other than methanol inducible promoters that have been characterized in *O. polymorph* [28], which is incompatible for pathway optimization under non-methanol medium. Furthermore, responsive promoters should make great sense for dynamically controlling cell factories [29,30]. Glucose responsive *GAL* and *HXT1* promoters in *S. cerevisiae* achieved higher (+)-valencene

Peer review under responsibility of KeAi Communications Co., Ltd.
* Corresponding author. Division of Biotechnology, Dalian Institute of Chemical Physics, Chinese Academy of Sciences, 457 Zhongshan Road, Dalian, 116023, PR China.
E-mail address: zhouyongjin@dicp.ac.cn (Y.J. Zhou).

https://doi.org/10.1016/j.synbio.2024.02.001
Received 12 January 2024; Received in revised form 1 February 2024; Accepted 4 February 2024
Available online 11 February 2024

production due to temporal separation of product formation from cell growth [31]. Fatty acid/acyl-CoA responsive promoters were also identified and drove higher metabolic flux to fatty alcohol biosynthesis [32].

Recently, nonconventional microorganisms have attracted much attention owing to some unique biochemical characteristics, including wide substrate spectrums, as well as tolerance to harsh conditions [33–35]. *Ogataea polymorpha* is supposed to be an ideal host for production of chemicals from diverse carbon sources, such as free fatty acids from glucose and xylose [36], 3-hydroxypropionate and fatty alcohol from methanol [37,38] and β-elemene from glucose [39]., Furthermore, there are well-established genome editing technologies [40,41] available for metabolic engineering of *O. polymorpha*. However, the limited promoter library, especially for responsive promoters, greatly hinders precise regulation of gene expression and pathway optimization in *O. polymorpha*.

In this study, we characterized 15 promoters in *O. polymorpha* based on transcriptional data and identified a series of constitutive promoters with strengths ranging from 0–55% of P_{GAP}, a constitutive promoter of glyceraldehyde-3-phosphate dehydrogenase gene. Furthermore, two growth phase-dependent promoters were also identified. Subsequently, two hybrid growth phase-dependent promoters were constructed, which had 2-fold increased activities compared to the wild-type promoters. Finally, these characterized promoters were used to rewire the central metabolism for improving the supply of acetyl-CoA, which achieved high level β-elemene production of 5.24 g/L with yield of 0.037 g/(g glucose) without compromising the cellular fitness, coupled with the phase-dependent expression of synthase module (*ERG20~LsLTC2* fusion) (see Fig. 1).

2. Results

2.1. Selecting candidate promoters by transcriptomic analysis

To expand the promoter library for precise metabolic engineering in *O. polymorpha*, wild-type strain was cultivated in glucose minimal medium and then collected at exponential phase and stationary phase for RNA-seq (Fig. 2A). FPKM (fragments per kilobase of exon model per million mapped reads) values are usually used for characterizing promoters [22,26], considering the positive correlation between the strengths of previously reported promoters (characterized by eGFP fluorescence intensities) [28,42] and FPKM values (Fig. S1A). On this basis, housekeeping gene actin (OGAPODRAFT_17014) with an average FPKM value of 1000 was used as reference, 12 candidate constitutive promoters from genes with FPKM≥3 $FPKM_{ACT}$ were selected. Also, 3 candidate responsive promoters were included, whose expression presented largely different FPKM values at different sampling times (Tables S1–2).

To minimize the promoter lengths for the convenience of constructing gene expression cassettes, the region between two neighboring genes [43,44] was defined as the promoter, despite 1000 bp upstream of the CDS region was commonly used as the promoter in *O. polymorpha* [28,42]. Particularly, for those promoters with lengths of less than 200 bp, or more than 1000 bp, 500 bp and 1000 bp upstream of the start codon were adopted as the promoters, respectively (Tables S1–2).

2.2. Promoter characterization by using fluorescent protein

Enhanced green fluorescent protein (eGFP) has been frequently used for promoter characterization in yeasts [22,28,42,44,45]. Therefore, the fluorescence intensities of eGFP driven by all promoter candidates were assayed at early (20 h) and late exponential phase (36 h), early (48 h) and late (72 h) stationary phase, respectively. As shown in Fig. 2B, these promoters possessed diverse strengths, among which Pro-Y4 showed the highest activity (55.2% of P_{GAP}), followed by Pro-Y7 and Pro-Y1 (around 30% of P_{GAP}). Surprisingly, Pro-Y3 and Pro-Y8 had nearly no detectable fluorescence signal, which were quite different from FPKM values. Pro-Y8 is the promoter of NADH-L-xylulose reductase gene (Table S1) and functional during xylose metabolism, which would be repressed under glucose medium. While Pro-Y3, the low fluorescence is out of our expectation with unknown reasons. Similar results about inconsistence between transcriptional and protein level were also reported in some

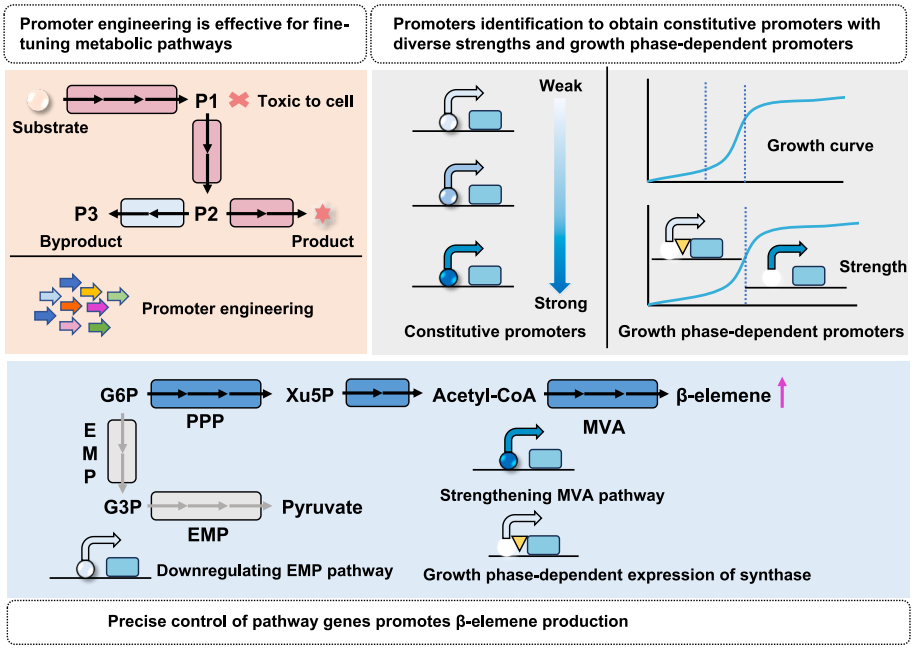

Fig. 1. Promoter identification improves the production of desired product through precise regulation of metabolic pathways. Chemicals with long and complex pathways require precise metabolic modulation, and promoter engineering is a powerful strategy. Therefore, constructing promoter library is important in the nonconventional yeast, *O. polymorpha*. We identified constitutive promoters and growth phase-dependent promoters for pathway optimization (weak promoters downregulated genes in EMP pathway, and strong constitutive promoters enhanced genes in MVA pathway, moreover, growth phase-dependent promoter was used for synthase expression) to achieve efficient production of β-elemene.

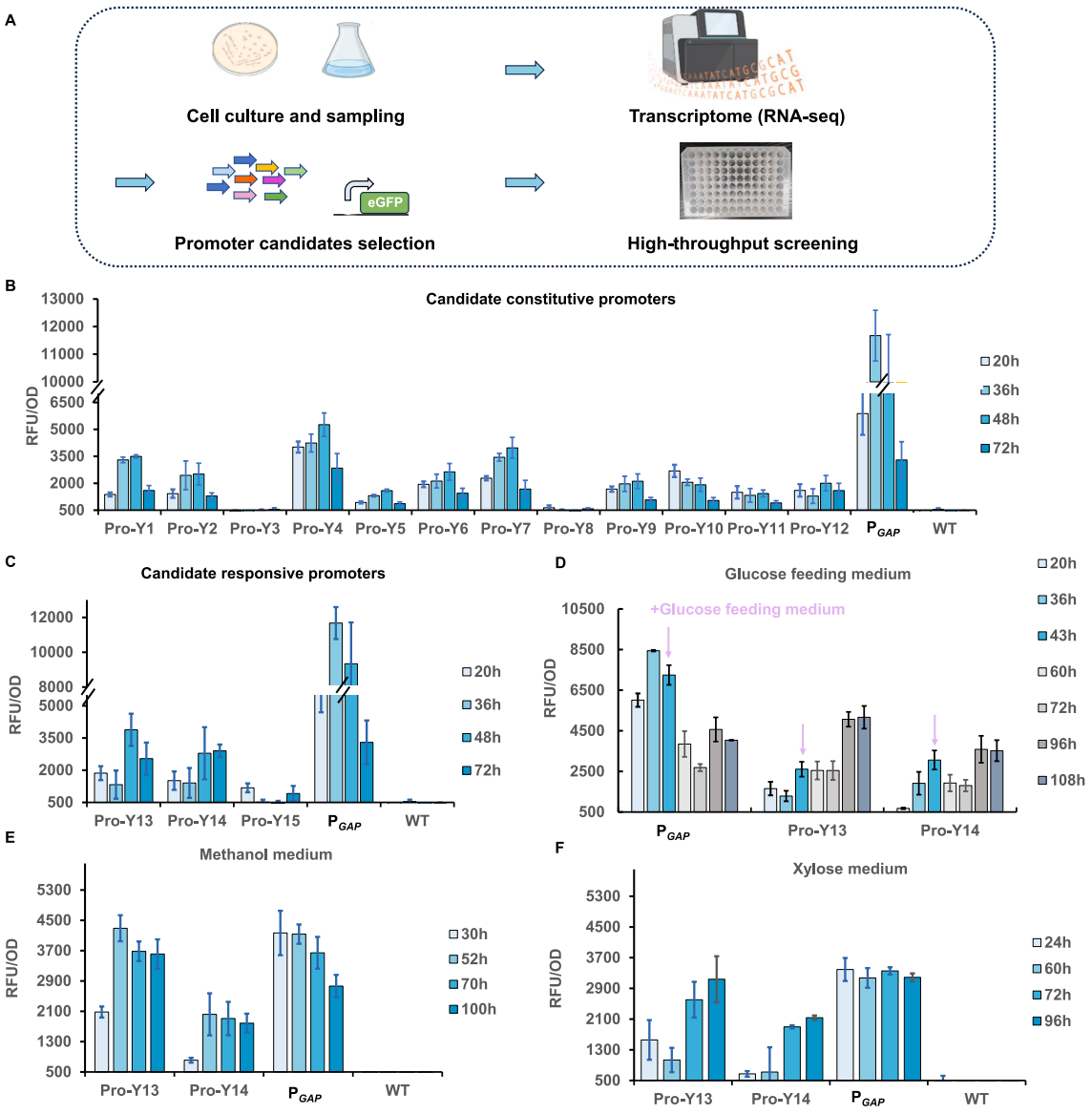

Fig. 2. Screening and characterizing constitutive and responsive promoters from *O. polymorpha*. **(A).** Schematic diagram of promoter characterization based on transcriptional data. Fluorescence intensities of candidate constitutive promoters **(B)** and responsive promoters **(C)** were detected in minimal medium with 20 g/L glucose. Fluorescence assay was conducted in 96 deep-well plate and the samples were taken at early (20 h) and late (36 h) exponential phase, early (48 h) and late (72 h) stationary phase. eGFP controlled by P_{GAP} was used as positive control, while strain without eGFP (WT) was used as negative control. Fluorescence intensities of candidate responsive promoters were evaluated under glucose feeding fermentation (**D**), 10 g/L methanol (**E**) or 10 g/L xylose (**F**) minimal medium in shake flasks. In the glucose feeding fermentation, glucose was fed into the medium at 43 h. The data showed in B and C was calculated from four biological replicates.

other genes [26]. Similar to the reported study [27], the fluorescence intensities of these constitutive promoters as well as P_{GAP} dramatically decreased at late stationary phase (Fig. 2B).

Promoters Pro-Y13 and Pro-Y14 showed responsive behaviors with growth phases, which showed low activities at early growth stage (20 h and 36 h), and had high activities at early stationary phase, and even late stationary phase when strength of P_{GAP} largely decreased (Fig. 2C, Fig. S1B). However, Pro-Y15 exhibited low fluorescence signals in the whole period (Fig. 2C). Considering the possible applications of responsive promoters in fed-batch fermentation, we investigated the influence of glucose feeding on the activities of Pro-Y13 and Pro-Y14. Feeding glucose into the medium at 43 h (Fig. S1C), the fluorescence signals of Pro-Y14 and P_{GAP} decreased, while at 96 h, the activities of Pro-Y13 and Pro-Y14 significantly increased (Fig. 2D). Pro-Y14, the promoter of a gene annotated as a putative transmembrane protein that involved in export of ammonia, which provides the major route for shuttling ammonium NH_4^+ and NH_3 [46]. Feeding fresh medium with sufficient ammonia resulted the repression of Pro-Y14 after 43 h. With strains growing and consuming of the ammonia after 72 h, the promoter functions again. Pro-Y13, the promoter of a heat shock protein gene, which was activated in response to stresses [47]. The accumulation of toxic metabolites under stationary phase, especially late stationary phase resulted higher cellular stress and activated the transcription of Pro-Y13 after 72 h. Thus, these two responsive promoters would be suitable for dynamic regulation of product biosynthesis in the fed-batch models.

Subsequently, we evaluated the performance of Pro-Y13 and Pro-Y14 in minimal medium with methanol or xylose as sole carbon sources, another two common substrates for *O. polymorpha*. The two promoters both showed similar profiles with those in glucose (Fig. 2E–F, Fig. S2). Interestingly, promoter P_{GAP} showed obviously lower activities in methanol and xylose medium than that in glucose (comparing Fig. 2C

with Fig. 2E–F), which might be caused by the low activity of glycolysis under methanol and xylose medium; whereas the activities of Pro-Y13 and Pro-Y14 were barely affected among different substrates. Since the expression profile of Pro-Y13 and Pro-Y14 were related to the cell growth, therefore, Pro-Y13 and Pro-Y14 could be defined as growth phase-dependent promoters [48], which were activated at stationary phase.

2.3. Engineering growth phase-dependent promoters

Although Pro-Y13 and Pro-Y14 were growth phase-dependent, the low activities in glucose (30% of P_{GAP}) limited their application in metabolic engineering (Fig. 2C). We thus tried to enhance the promoter activity by engineering the upstream activation sequence (UAS). Based on the prediction of the putative core promoters and transcriptional binding sites, we truncated Pro-Y13 and Pro-Y14 into 5 and 6 parts, respectively (Fig. 3A and B), and then characterized these truncated promoters by using eGFP. Pro-Y13-S1 and Pro-Y14-S1 exhibited nearly no fluorescence, which was defined as the core promoter region. Considering the gradually increased fluorescence signals of the truncated promoters S2 and S3, two UAS elements (UAS1 and UAS2) were identified in regions S2–S1 and S3–S2 in both Pro-Y13 and Pro-Y14 (Fig. 3A and B).

Subsequently, we constructed hybrid promoters by tandem fusing UAS region (Fig. 3C). Hybrid promoters Phy3 consisting of core promoter region of Pro-Y13 and two tandem $UAS1^{Y13}$+$UAS2^{Y13}$ regions and Phy4 consisting of core promoter region of Pro-Y14 and tandem fusion of $UAS1^{Y13}$+$UAS2^{Y13}$ and $UAS1^{Y14}$+$UAS2^{Y14}$ regions were constructed (Fig. 3C). Both hybrids showed 2-fold increase in activities than those of wild-type Pro-Y13 and Pro-Y14, which reached almost 50% of the strength of P_{GAP} at 48 h. More importantly, they had high activities at late stationary phase, which outperformed P_{GAP} at 72 h (Fig. 3C). Other methods like adding copy numbers of UAS regions [49] or creating mutant UAS library [50] could also be employed for further enhancing the promoter activity.

2.4. Promoter engineering for β-elemene production

Previously, we showed that reconstruction of PK-PTA pathway for enhancing acetyl-CoA supply, failed in improving β-elemene production in *O. polymorpha* [39]. We speculated that the supply of xylulose-5 phosphate (Xu5P) from PPP might be limited towards PK-PTA pathway for acetyl-CoA biosynthesis (Fig. 4A). We thus tried to enhance the PPP flux by down-regulating glycolytic pathway (EMP) in an engineered strain YY-122 with overexpression of *ERG10* and *ERG13*. Genes at the key nodes, including phosphofructokinase (*PFK1, PFK2*), glucose-6-phosphate isomerase (*PGI1*), fructose-bisphosphate aldolase (*FBA*), and *GAP*, were regulated by using different promoters. Down-regulating the rate-limiting gene *GAP*, by replacing the native promoter with promoters with gradually decreased activities, significantly

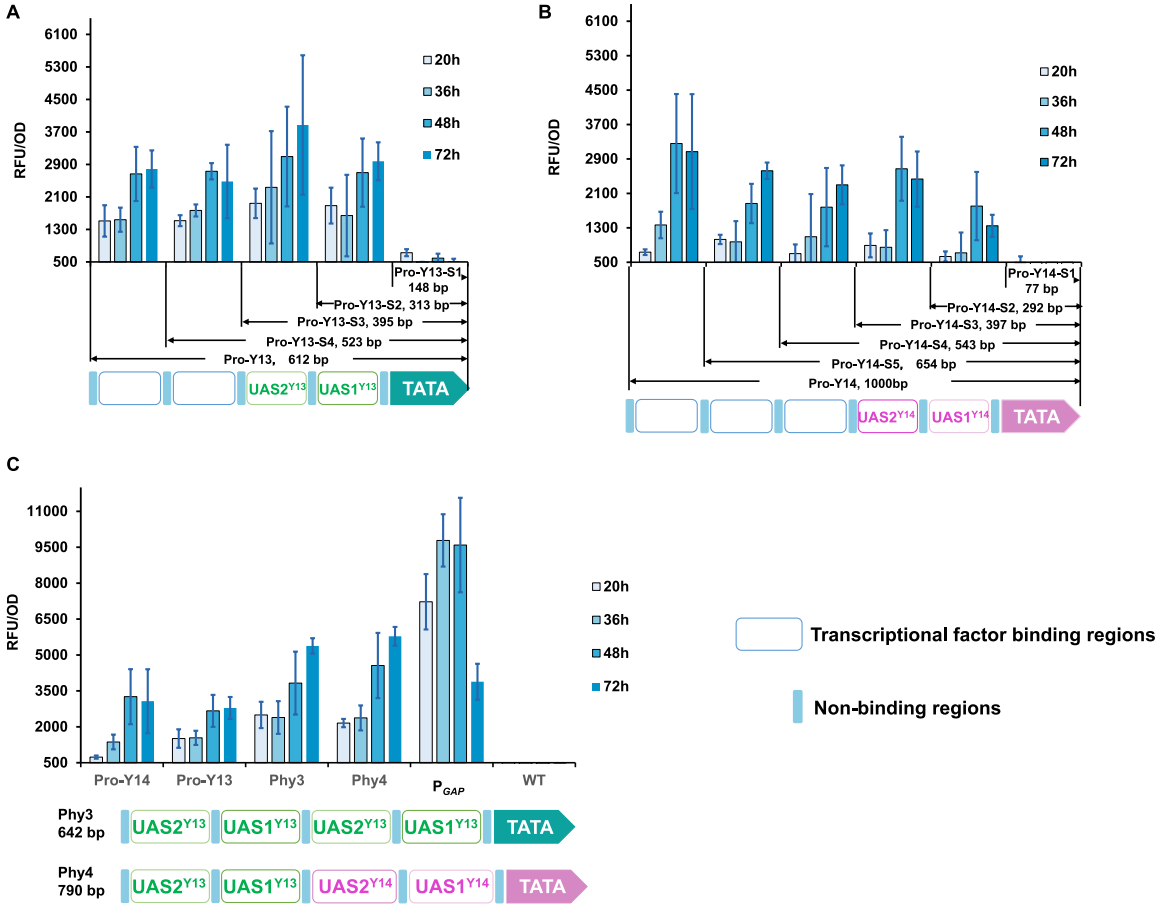

Fig. 3. Promoter engineering enhanced the strengths of two growth phase-dependent promoters. (A)–(B). Identification of core promoter region and upstream activation sequence (UAS) in growth phase-dependent promoters Pro-Y13 and Pro-Y14. Promoters were truncated based on bioinformatics prediction, and each truncated promoter was separated by a transcriptional factor binding region. All the truncated promoters were evaluated by eGFP signals. **(C).** Characterization of hybrid promoters. Hybrid promoters were constructed by tandem fusing UAS regions. All promoters were evaluated by fluorescence values under glucose minimal medium in 96 deep-well plate, and the samples were taken at early (20 h) and late (36 h) exponential phase, early (48 h) and late (72 h) stationary phase. The data were calculated from four biological replicates.

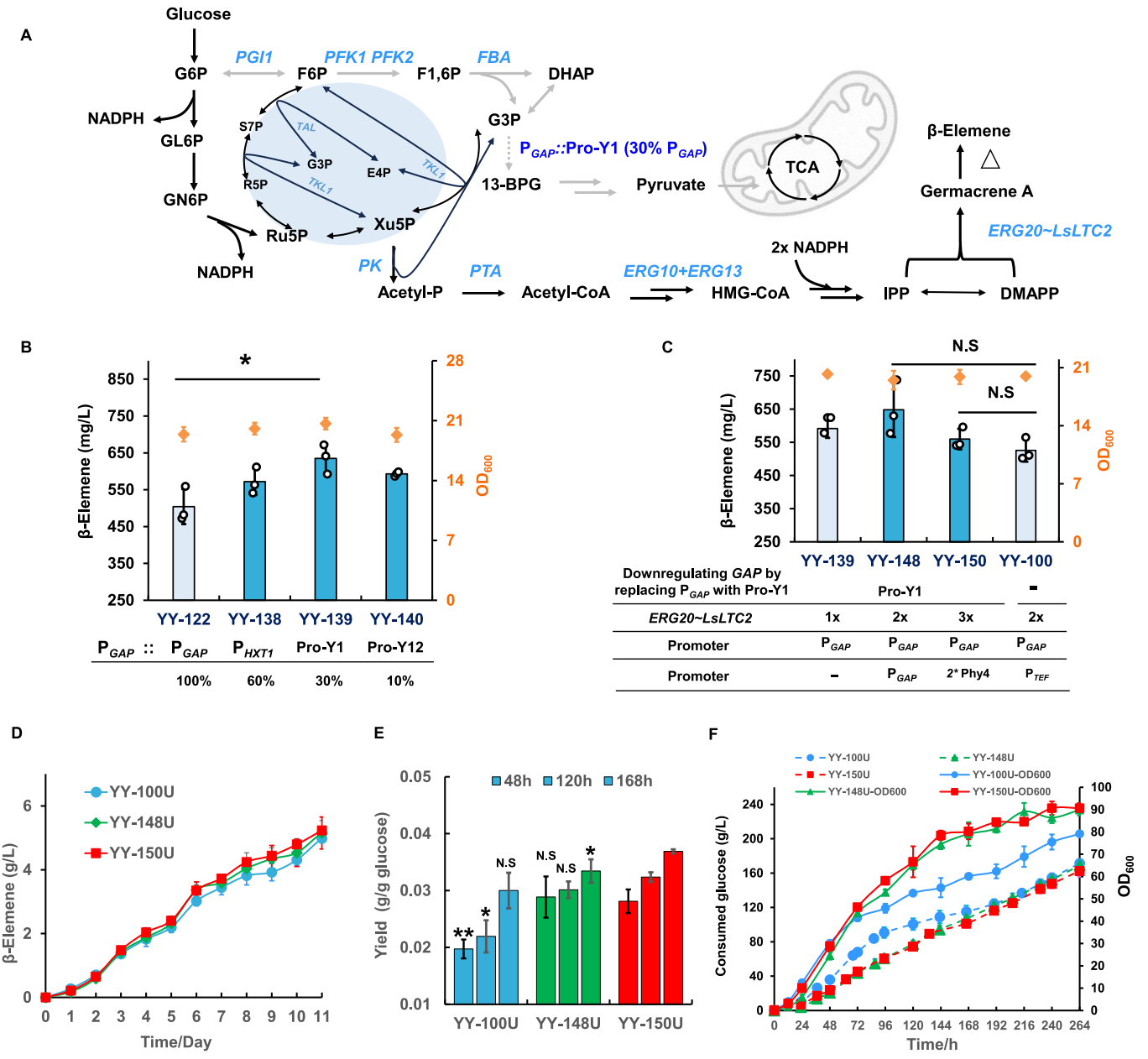

Fig. 4. Precise metabolic regulation by promoter engineering promoted β-elemene production. **(A).** Schematic of modulating the expression of genes in EMP pathway drives the flux into PPP. **(B)–(C).** β-elemene production by engineered strains under shake flasks fermentation. **(D)–(F).** β-elemene production under fed-batch fermentation in shake flasks. Fed-batch fermentation in shake flasks was performed using Delft minimal medium. During fermentation, β-elemene titer **(D)** and cell growth (OD_{600}) **(F)**, consumed glucose **(F)** was monitored. In particular, the yields of β-elemene were calculated at 48 h, 120 h, 168 h, respectively **(E)**. The data displayed in fed-batch fermentation was calculated from four biological replicates. Error bars were analyzed by the Student's t-test (two-sample, two-tailed; * *P*-value <0.05, ** *P*-value <0.01, N.S represents no significant difference).

promoted the β-elemene production. Replacing P_{GAP} with Pro-Y1 (30% strength of P_{GAP}) achieved the highest improvement of β-elemene titer (635 mg/L, Fig. 4B), with no detectable influence on cell growth (Fig. S3A). Downregulating *GAP* contributed to the enhanced production, suggesting that the restricted EMP drove the increased PPP flux for acetyl-CoA supply by PK-PTA pathway. However, the repression of *PFK1,2* (Figs. S3B–C), *PGI1* (Fig. S3D), and *FBA* (Fig. S3E) with either weaker promoters or degradation peptide ($CLN2^{PEST}$) had no influence on β-elemene production and cell biomass. We failed to get the strains with extremely low expression of *FBA* with Pro-Y8 and $CLN2^{PEST}$, which might result in cell death (Fig. S3D). More precise regulation by using broader strength of promoters or creating combinatorial library for EMP pathway optimization might be helpful for improving β-elemene production.

We previously demonstrated that the enhanced expression of *ERG20~LsLTC2* fusion would drive the flux to β-elemene production in engineered strain *O. polymorpha* [39]. We thus tried to integrate more copies of *ERG20~LsLTC2* in the YY-139 genome by using constitutive promoter P_{GAP} or hybrid promoter Phy4. Considering the relatively low activities of hybrid promoter Phy4 (Fig. 3C), we integrated two copies of *ERG20~LsLTC2* driven by promoter Phy4 (strain YY-150). Integrating another copy of *ERG20~LsLTC2* controlled by P_{GAP} (YY-148) slightly increased the titer by 10%–650 mg/L compared with the parent strain YY139. Unfortunately, the *ERG20~LsLTC2* fusion driven by Phy4 had no contribution to β-elemene production. All engineered strains constructed in this study showed the superior performance in β-elemene

production compared with the previously engineered strain YY100 [39], which demonstrated the significance of precise metabolic regulation by promoter engineering (Fig. 4C).

The growth dependent hybrid promoter Phy4 (Fig. 3C) might be beneficial for continuous expression in fed-batch fermentation. We evaluated the β-elemene production of prototrophic strains YY-150U, YY-148U and control strain YY-100U [39] under fed-batch fermentation in shake flasks, since prototrophic strains are more stable without compromise the cell growth [51]. After 11 days cultivation, YY150U had the highest β-elemene titer of 5.24 g/L (Fig. 4D) and yield of 0.037 g/(g glucose) (Fig. 4E), which showed that Phy4 performed better than P_{GAP} in expressing *ERG20~LsLTC2*. Both YY-148U and YY-150U with downregulated *GAP* accumulated more biomass than YY-100U, and YY-150U reached OD_{600} of 90 (Fig. 4F). Interestingly, YY-148U and YY-150U had lower glucose consumption rates than YY-100U, especially in the first 96 h (Fig. 4F), probably owing to the reduced glycolysis flux.

3. Discussion

Construction of robust cell factories requires extensive metabolic engineering to achieve high titers, yields, and productivities. Promoter engineering is a feasible approach for regulating gene expression in metabolic rewiring. In this study, we expanded the promoter library of *O. polymorpha* by transcriptomic analysis and fluorescence analysis during the whole growth process. This strategy enabled to identify 13 constitutive promoters with strengths ranging from 0–55% of P_{GAP} and 2 growth phase-dependent promoters with high expression at stationary phase.

Although FPKM values from transcriptomics are commonly applied in promoter screening [22,26], it should be noted that the promoter strengths may not always be positively related to the FPKM values. For example, P_{TEF1}, commonly regarded as a strong constitutive promoter [52], shows relatively low FPKM value (<1000). Also, the expression level of a specific gene largely depends on its length [53], which may partially explain our phenomenon that promoters from genes with high FPKM values only had moderate fluorescence signals.

The phase-dependent promoters showed excellent performance under glucose, methanol, xylose and especially, glucose feeding conditions. Furthermore, the expression profiles of Pro-Y13 and Pro-Y14 were well correlated with their gene function. We also constructed two hybrid promoters with a two-fold increase in activities by identifying and integrating UAS regions. Tandem UAS region has been proved as an efficient strategy to increase the promoter strengths [54,55], but the increased leaky expression needs further exploration. Compared with other dynamic systems responsive to extracellular inducer like copper [56], estrogen [57], metabolites malonyl-CoA [58,59], and environmental factors like blue light [60] or temperature [61], the growth phase-dependent promoters we have identified are more convenient and inexpensive to use.

Acetyl-CoA is an important precursor for biosynthesis of a variety of chemicals such as isoprenoids, fatty acids, 3-hydroxypropionic acid [16,36,62]. Thus, enhancing the acetyl-CoA supply by metabolic rewiring is a feasible approach for efficient biosynthesis. However, modulating the cellular metabolism in nonconventional yeast such as *O. polymorpha* is still challenging, and the strategies learned from *S. cerevisiae* and *Yarrowia lipolytica* have limited effects [37,39]. Here, we used the identified promoters to drive more carbon flux for acetyl-CoA supply in a PK-PTA pathway by moderate repression of the key EMP gene *GAP*, which significantly promoted the production of both β-elemene and biomass. The increased efficiency in glucose utilization under fed-batch fermentation also led to the higher yields. However, we here only modulated single gene in EMP pathway by using several promoters, and further comprehensive optimization for pathway genes by creating a combinatorial library [17,18] should be beneficial for improve bioproduction.

In summary, we expanded the promoter library for precise optimization and regulation of metabolic pathway in yeast *O. polymorpha*. The final engineered strain achieved higher biomass, titer and yield, which could be applied for efficient production of other chemicals in the future.

4. Materials and methods

4.1. Strains, plasmids and medium

All strains used are listed in Table S3. Strain Ku80ΔL (with a copy of the integrated *CAS9* gene, a disrupted *ku80* gene) was used for RNA-Seq, and strains used for promoter characterization were conducted in strain JQCR03L (Ku80L with an overexpressed gene *SAE2*). Strains used for β-elemene production were constructed from strain YY-98 (Ku80L with optimized MVA pathway and PPP pathway) [39]. gRNA expression plasmids were constructed according to previous descriptions [63] and are listed in Table S4. Related primers (Table S5) were synthesized by Sangon Biotech (Shanghai, China).

YPD medium containing 10 g/L yeast extract, 20 g/L peptone and 20 g/L glucose was used for cultivation of seed cells. Synthetic dropout (SD) solid medium (6.7 g/L yeast nitrogen base, 20 g/L glucose and 18–20 g/L agar) was used for selection of recombinant strains. For gRNA removal, strains were cultivated in YPD+5-FOA plates containing YPD, 18 g/L agar and 1 g/L 5-fluoroorotic acid. Delft minimal medium (pH 5.6) was used for fermentation and contained 2.5 g/L $(NH_4)_2SO_4$, 14.4 g/L KH_2PO_4, 0.5 g/L $MgSO_4{\cdot}7H_2O$, 20 g/L glucose or 10 g/L xylose or 10 g/L methanol, 2 mL/L trace metals (3.0 g/L $FeSO_4{\bullet}7H_2O$, 4.5 g/L $ZnSO_4{\bullet}7H_2O$, 4.5 g/L $CaCl_2{\bullet}2H_2O$, 1 g/L $MnCl_2{\bullet}4H_2O$, 300 mg/L $CoCl_2{\bullet}6H_2O$, 300 mg/L $CuSO_4{\bullet}5H_2O$, 400 mg/L $Na_2MoO_4{\bullet}2H_2O$, 1 g/L H_3BO_3, 100 mg/L KI, 19 g/L $Na_2EDTA{\bullet}2H_2O$) and 1 mL/L vitamin solution (50 mg/L D-biotin, 1.0 g/L D-pantothenic acid hemicalcium salt, 1.0 g/L thiamin-HCl, 1.0 g/L pyridoxin-HCl, 1.0 g/L nicotinic acid, 0.2 g/L 4-aminobenzoic acid, 25 g/L m-inositol), supplemented with 20 mg/L (for glucose and xylose medium) or 60 mg/L (for methanol medium) uracil if needed.

Escherichia coli DH5α was used for amplificating of plasmids and cultivated in LB medium containing 10 g/L tryptone, 5 g/L yeast extract, and 10 g/L NaCl, and 100 μg/mL ampicillin for plasmids maintenance.

All reagents were purchased from Sangon Biotech (Shanghai, China), except standard β-caryophyllene (#C832338; CAS: 87-44-5) and β-elemene (#E885859; CAS:515-13-9), which were purchased from Macklin.

4.2. RNA-seq assays

Ku80ΔL was first streaked on YPD plates and grown for 3 days, and then single colonies were picked and precultured in 10 mL of YPD medium in 50 mL tubes. After 12–16 h of cultivation, yeast cells were collected and washed once with Delft minimal medium, then the cells were collected and resuspended in Delft minimal medium and subsequently, transferred into 50 mL of Delft minimal medium in a 250 mL shake flask, with 20 g/L glucose as sole carbon source, and cultivated at 37 °C and 220 rpm. Samples were collected at 24 h (exponential phase) and 36 h (stationary phase). Cells were centrifuged at 2000 g, 5 min and washed twice with water. Yeast cells were stored at −80 °C and then sent for RNA-Seq (Biozeron, Shanghai, China).

4.3. Selection of candidate promoters

According to the transcriptional data, genes with FPKM (fragments per kilobase million) values ≥ 3 $FPKM_{ACT}$ were selected. Then promoters of these genes were acquired as the region between start codon to the stop codon of the upstream gene [43,44], for those promoters with lengths of less than 200 bp, or more than 1000 bp, 500 bp and 1000 bp upstream of the start codon were adopted as the promoters. The sequences of promoters are listed in Table S6.

4.4. Genetic Manipulation

According to previous reports [39,40,64], the expression cassettes containing 1000 bp upstream and downstream homologous arms, a promoter, a structural gene and a terminator were constructed by overlap extension PCR, and strains in this study were constructed by CRISPR-Cas9 genome editing technology, with 500 ng sgRNA and 500 ng donor DNA transformed into competent cells using electro-transformation method.

4.5. Promoter engineering

Pro-Y13 and Pro-Y14 were truncated according to online prediction of core promoter through BDGP: Neural Network Promoter Prediction (fruitfly.org) [65] and transcription factors binding sites through Alibaba2 (gene-regulation.com). And then the truncated promoters were evaluated to obtain core promoters and UAS (upstream activating sequence) regions. After acquiring UAS regions, we constructed hybrid promoters through overlap extension PCR.

4.6. Fluorescence assay

Strains were first streaked on YPD plates and grown for 3 days, and then single colonies were picked and precultured in YPD. For 96 deep-well plate cultivation, 10 μL of the seed culture was inoculated into 96 deep-well plate containing 290 μL Delft minimal medium and 20 g/L glucose as the carbon source (approximately 0.2 of the initial OD_{600}). After 30–36 h of cultivation at 37 °C and 600 rpm, 30 μL seed culture was inoculated into 96 deep-well plates containing 270 μL Delft minimal medium and 20 g/L glucose as the carbon source (approximately 0.4 of the initial OD_{600}) and cultivated at 37 °C and 600 rpm. For shake flasks cultivation, seed cells were collected and washed once, then resuspended in Delft minimal medium and subsequently, transferred into 15 mL Delft minimal medium containing 20 g/L glucose or 10 g/L xylose or 10 g/L methanol as sole carbon source in 100 mL shake flasks. For glucose feeding medium, when the concentration of glucose in the medium was lower than 5 g/L (at 43 h), the cells were fed with 1 mL 500 g/L glucose feeding solution containing 12.5 g/L $(NH_4)_2SO_4$, 72 g/L KH_2PO_4, 2.5 g/L $MgSO_4 \bullet 7H_2O$, 10 × trace metals, 5 × vitamin solution and 150 μL 2 g/L Uracil. Samples were collected at early and late exponential phase, early and late stationary phase. At each sampling time, cells were collected and centrifuged, and then the cell pellets were washed twice with H_2O, and diluted to $OD_{600} = 1$. Then, the cell suspensions were tested with a Tecan SPARK microplate reader (Tecan, Switzerland) for test as previously described [63].

4.7. Evaluation of β-elemene producing strain

The corrected transformants with gRNA removal were evaluated in 15 mL of Delft minimal medium containing 20 g/L glucose in 100 mL shake flasks, and the biomass and the extraction and analysis of β-elemene were performed as described in previous report [39]. Briefly, after 72–96 h of cultivation, the biomass was measured from the OD_{600}, and the organic layer was collected for product analysis. The β-elemene amounts were calculated by external standard calibration and corrected by using the internal standard β-caryophyllene. The final titers were calculated from the concentration ratio. A GC-FID instrument (Focus GC, Thermo Fisher Scientific) equipped with a Zebron ZB-5MS GUARDIAN capillary column (30 m × 0.25 mm × 0.25 μm) was used for quantification.

Fed-batch fermentation in shake flasks was conducted as previously reported [39] by using 50 mL of Delft minimal medium in 250 mL shake flasks, with 20% dodecane added for two-phase fermentation. The strains were precultured in YPD medium, and then cells were collected and inoculated into fermentation media at an initial OD_{600} of 0.4. Samples were taken every 24 h to measure product titers and the OD_{600}. The pH of the culture was adjusted to 5–6 with 4 M KOH every 24 h. During the fed-batch process, residual glucose was detected to determine the feeding rates. When the concentration of glucose in the medium was lower than 5 g/L, the cells were fed with 1–2 mL 500 g/L glucose feeding solution containing 12.5 g/L $(NH_4)_2SO_4$, 72 g/L KH_2PO_4, 2.5 g/L $MgSO_4 \bullet 7H_2O$, 10 × trace metals, and 5 × vitamin solution. The glucose concentration was determined by using an SBA40D biosensor (Biology Institute of Shandong Academy of Sciences, Shandong, China) according to the instruction manual.

4.8. Statistical analysis

Statistical analysis was performed by Microsoft Excel software using a two sample, two-tailed *t*-test analysis of variance hypothesis. Significant differences are marked as $^*P < 0.05$, $^{**}P < 0.01$ and $^{***}P < 0.001$. All data are presented as mean ± s.e.m. The number of biologically independent samples for each panel was three unless otherwise stated in the figure legends.

Declarations of interest

The authors declare no conflict of interest.

CRediT authorship contribution statement

Min Ye: Methodology, Investigation, Writing – original draft. **Jiaoqi Gao:** Methodology, Resources, Project administration, Funding acquisition, Writing – review & editing. **Jingjing Li:** Investigation, Writing – review & editing. **Wei Yu:** Investigation, Writing – review & editing. **Fan Bai:** Funding acquisition. **Yongjin J. Zhou:** Conceptualization, Supervision, Project administration, Funding acquisition, Writing – review & editing.

Declaration of competing interest

Yongjin J. Zhou is an Associate Editorfor Synthetic and Systems Biotechnology and was not involved in the editorial review or the decision to publish this article.

Acknowledgments

This research was supported by the National Key Research and Development Project (2023YFC3503900), and Liaoning Distinguished Scholar Program (2023JH6/100500001)

Appendix A. Supplementary data

Supplementary data to this article can be found online at https://doi.org/10.1016/j.synbio.2024.02.001.

References

[1] Wang C, Pfleger BF, Kim S-W. Reassessing *Escherichia coli* as a cell factory for biofuel production. Curr Opin Biotechnol 2017;45:92–103.
[2] Liu Y, Cruz-Morales P, Zargar A, Belcher MS, Pang B, Englund E, et al. Biofuels for a sustainable future. Cell 2021;184(6):1636–47.
[3] Zhou YJ, Buijs NA, Zhu Z, Qin J, Siewers V, Nielsen J. Production of fatty acid-derived oleochemicals and biofuels by synthetic yeast cell factories. Nat Commun 2016;7:11709–19.
[4] Li M, Hou F, Wu T, Jiang X, Li F, Liu H, et al. Recent advances of metabolic engineering strategies in natural isoprenoid production using cell factories. Nat Prod Rep 2020;37(1):80–99.
[5] Pramastya H, Song Y, Elfahmi EY, Sukrasno S, Quax WJ. Positioning Bacillus subtilis as terpenoid cell factory. J Appl Microbiol 2020;130(6):1839–56.
[6] Belcher MS, Mahinthakumar J, Keasling JD. New frontiers: harnessing pivotal advances in microbial engineering for the biosynthesis of plant-derived terpenoids. Curr Opin Biotechnol 2020;65:88–93.
[7] Yang H, Zhang K, Shen W, Xia Y, Li Y, Chen X. Boosting production of cembratriene-ol in *Saccharomyces cerevisiae* via systematic optimization. Biotechnol J 2024;19(1):e2300324..

[8] Chrzanowski G. Saccharomyces cerevisiae-an interesting producer of bioactive plant polyphenolic metabolites. Int J Mol Sci 2020;21(19):7343–61.
[9] Carvalho A, Hansen EH, Kayser O, Carlsen S, Stehle F. Designing microorganisms for heterologous biosynthesis of cannabinoids. FEMS Yeast Res 2017;17(4):1–11.
[10] Srinivasan P, Smolke CD. Biosynthesis of medicinal tropane alkaloids in yeast. Nature 2020;585(7826):614–9.
[11] Ajikumar PK, Xiao W-H, Keith E, Tyo J, Wang Y, Simeon F, et al. Isoprenoid pathway optimization for taxol precursor overproduction in *Escherichia coli*. Science 2010;330:70–4.
[12] Alper H, Fischer C, Nevoigt E, Stephanopoulos G. Tuning genetic control through promoter engineering. Proc Natl Acad Sci U S A 2005;102:12678–83.
[13] Chen X, Gao C, Guo L, Hu G, Luo Q, Liu J, et al. DCEO biotechnology: tools to design, construct, evaluate, and optimize the metabolic pathway for biosynthesis of chemicals. Chem. Rev 2017;118(1):4–72.
[14] Johari YB, Scarrott JM, Pohle TH, Liu P, Mayer A, Brown AJ, et al. Engineering of the CMV promoter for controlled expression of recombinant genes in HEK293 cells. Biotechnol J 2022;17(8):e2200062.
[15] Li M, Kildegaard KR, Chen Y, Rodriguez A, Borodina I, Nielsen J. De novo production of resveratrol from glucose or ethanol by engineered *Saccharomyces cerevisiae*. Metab Eng 2015;32:1–11.
[16] Yu T, Zhou YJ, Huang M, Liu Q, Pereira R, David F, et al. Reprogramming yeast metabolism from alcoholic fermentation to lipogenesis. Cell 2018;174(6):1549–58.
[17] Mukherjee M, Blair RH, Wang ZQ. Machine-learning guided elucidation of contribution of individual steps in the mevalonate pathway and construction of a yeast platform strain for terpenoid production. Metab Eng 2022;74:139–49.
[18] Yamada R, Wakita K, Ogino H. Global metabolic engineering of glycolytic pathway via multicopy integration in *Saccharomyces cerevisiae*. ACS Synth Biol 2017;6(4):659–66.
[19] Zhou L, Wang Y, Han L, Wang Q, Liu H, Cheng P, et al. Enhancement of patchoulol production in *Escherichia coli* via multiple engineering strategies. J Agric Food Chem 2021;69(27):7572–80.
[20] Shimazaki S, Yamada R, Yamamoto Y, Matsumoto T, Ogino H. Building a machine-learning model to predict optimal mevalonate pathway gene expression levels for efficient production of a carotenoid in yeast. Biotechnol J 2023;19(1):e2300285.
[21] Sun J, Shao Z, Zhao H, Nair N, Wen F, Xu JH, et al. Cloning and characterization of a panel of constitutive promoters for applications in pathway engineering in *Saccharomyces cerevisiae*. Biotechnol Bioeng 2012;109(8):2082–92.
[22] Gao S, Zhou H, Zhou J, Chen J. Promoter-library-based pathway optimization for efficient (2S)-Naringenin production from p-coumaric acid in *Saccharomyces cerevisiae*. J Agric Food Chem 2020;68(25):6884–91.
[23] Peng B, Williams TC, Henry M, Nielsen LK, Vickers CE. Controlling heterologous gene expression in yeast cell factories on different carbon substrates and across the diauxic shift: a comparison of yeast promoter activities. Microb Cell Fact 2015;14:91–101.
[24] Cao L, Li J, Yang Z, Hu X, Wang P. A review of synthetic biology tools in *Yarrowia lipolytica*. World J Microbiol Biotechnol 2023;39(5):129–46.
[25] Wang C, Lin M, Yang Z, Lu X, Liu Y, Lu H, et al. Characterization of the endogenous promoters in *Yarrowia lipolytica* for the biomanufacturing applications. Process Biochem 2023;124:245–252..
[26] Dou W, Zhu Q, Zhang M, Jia Z, Guan W. Screening and evaluation of the strong endogenous promoters in *Pichia pastoris*. Microb Cell Fact 2021;20(1):156–68.
[27] Cai P, Duan X, Wu X, Gao L, Ye M, Zhou YJ. Recombination machinery engineering facilitates metabolic engineering of the industrial yeast *Pichia pastoris*. Nucleic Acids Res 2021;49(13):7791–805.
[28] Zhai X, Ji L, Gao J, Zhou YJ. Characterizing methanol metabolism-related promoters for metabolic engineering of *Ogataea polymorpha*. Appl Microbiol Biotechnol 2021;105(23):8761–9.
[29] Hartline CJ, Schmitz AC, Han Y, Zhang F. Dynamic control in metabolic engineering: theories, tools, and applications. Metab Eng 2021;63:126–40.
[30] Shen X, Wang J, Li C, Yuan Q, Yan Y. Dynamic gene expression engineering as a tool in pathway engineering. Curr Opin Biotechnol 2019;59:122–9.
[31] Ye Z, Huang Y, Shi B, Xiang Z, Tian Z, Huang M, et al. Coupling cell growth and biochemical pathway induction in *Saccharomyces cerevisiae* for production of (+)-valencene and its chemical conversion to (+)-nootkatone. Metab Eng 2022;72:107–15.
[32] Gao N, Gao J, Yu W, Kong S, Zhou YJ. Spatial–temporal regulation of fatty alcohol biosynthesis in yeast. Biotechnol Biofuels 2022;15(1):141–2.
[33] Li J, Rong L, Zhao Y, Li S, Zhang C, Xiao D, et al. Next-generation metabolic engineering of non-conventional microbial cell factories for carboxylic acid platform chemicals. Biotechnol Adv 2020;43:107605–28.
[34] Sun L, Alper HS. Non-conventional hosts for the production of fuels and chemicals. Curr Opin Chem Biol 2020;59:15–22.
[35] Karim A, Gerliani N, Aider M. *Kluyveromyces marxianus*: an emerging yeast cell factory for applications in food and biotechnology. Int J Food Microbiol 2020;333:108818–42.
[36] Gao J, Yu W, Li Y, Jin M, Yao L, Zhou YJ. Engineering co-utilization of glucose and xylose for chemical overproduction from lignocellulose. Nat Chem Biol 2023;19(12):1524–31.
[37] Yu W, Gao J, Yao L, Zhou YJ. Bioconversion of methanol to 3-hydroxypropionate by engineering *Ogataea polymorpha*. Chinese J Catal 2023;46:84–90.
[38] Zhai X, Gao J, Li Y, Grininger M, Zhou YJ. Peroxisomal metabolic coupling improves fatty alcohol production from sole methanol in yeast. Proc Natl Acad Sci U S A 2023;120(12):e2220816120.
[39] Ye M, Gao J, Zhou YJ. Global metabolic rewiring of the nonconventional yeast *Ogataea polymorpha* for biosynthesis of the sesquiterpenoid beta-elemene. Metab Eng 2023;76:225–31.
[40] Gao J, Gao N, Zhai X, Zhou YJ. Recombination machinery engineering for precise genome editing in methylotrophic yeast *Ogataea polymorpha*. iScience 2021;24(3):102168–73.
[41] Wang L, Deng A, Zhang Y, Liu S, Liang Y, Bai H, et al. Efficient CRISPR–Cas9 mediated multiplex genome editing in yeasts. Biotechnol Biofuels 2018;11(1):277–93.
[42] Yan C, Yu W, Zhai X, Yao L, Guo X, Gao J, et al. Characterizing and engineering promoters for metabolic engineering of *Ogataea polymorpha*. Synth Syst Biotechnol 2022;7(1):498–505.
[43] Kristiansson E, Thorsen M, Tamas MJ, Nerman O. Evolutionary forces act on promoter length: identification of enriched cis-regulatory elements. Mol Biol Evol 2009;26(6):1299–307.
[44] Vogl T, Sturmberger L, Kickenweiz T, Wasmayer R, Schmid C, Hatzl AM, et al. A toolbox of diverse promoters related to methanol utilization: functionally verified parts for heterologous pathway expression in *Pichia pastoris*. ACS Synth Biol 2016;5(2):172–86.
[45] Portela RM, Vogl T, Kniely C, Fischer JE, Oliveira R, Glieder A. Synthetic core promoters as universal parts for fine-tuning expression in different yeast species. ACS Synth Biol 2017;6(3):471–84.
[46] Ludewig U, Neuhäuser B, Dynowski M. Molecular mechanisms of ammonium transport and accumulation in plants. FEBS Lett 2007;581(12):2301–8.
[47] Hu C, Yang J, Qi Z, Wu H, Wang B, Zou F, et al. Heat shock proteins: biological functions, pathological roles, and therapeutic opportunities. MedComm 2022;3(3):e161–99.
[48] Yang S, Du G, Chen J, Kang Z. Characterization and application of endogenous phase-dependent promoters in *Bacillus subtilis*. Appl Microbiol Biotechnol 2017;101(10):4151–61.
[49] Blazeck J, Liu L, Redden H, Alper H. Tuning gene expression in *Yarrowia lipolytica* by a hybrid promoter approach. Appl Environ Microbiol 2011;77(22):7905–14.
[50] Li S, Ma L, Fu W, Su R, Zhao Y, Deng Y. Programmable synthetic upstream activating sequence library for fine-tuning gene expression levels in *Saccharomyces cerevisiae*. ACS Synth Biol 2022;11(3):1228–39.
[51] Yan C, Gao N, Cao X, Yao L, Zhou YJ, Gao J. Auxotrophs compromise cell growth and fatty acid production in *Saccharomyces cerevisiae*. Biotechnol J 2023;18(4):e2200510.
[52] Rebello S, Abraham A, Madhavan A, Sindhu R, Binod P, Karthika Bahuleyan A, et al. Non-conventional yeast cell factories for sustainable bioprocesses. FEMS Microbiol Lett 2018;365(21):1–9.
[53] Tuller T, Ruppin E, Kupiec M. Properties of untranslated regions of the *S. cerevisiae* genome. BMC Genom 2009;10:391–402.
[54] Liu Q, Song L, Peng Q, Zhu Q, Shi X, Xu M, et al. A programmable high-expression yeast platform responsive to user-defined signals. Sci Adv 2022;8:1–14.
[55] Zhu Q, Liu Q, Yao C, Zhang Y, Cai M. Yeast transcriptional device libraries enable precise synthesis of value-added chemicals from methanol. Nucleic Acids Res 2022;50(17):10187–99.
[56] Labbe S, Thiele DJ. Copper ion inducible and repressible promoter systems in yeast. Meth Enzymol 1999;306:145–53.
[57] Perez-Pinera P, Han N, Cleto S, Cao J, Purcell O, Shah KA, et al. Synthetic biology and microbioreactor platforms for programmable production of biologics at the point-of-care. Nat Commun 2016;7:12211–20.
[58] Li S, Si T, Wang M, Zhao H. Development of a synthetic malonyl-CoA sensor in *Saccharomyces cerevisiae* for intracellular metabolite monitoring and genetic screening. ACS Synth Biol 2015;4(12):1308–15.
[59] Wen J, Tian L, Xu M, Zhou X, Zhang Y, Cai M. A synthetic malonyl-CoA metabolic oscillator in *komagataella phaffii*. ACS Synth Biol 2020;9(5):1059–68.
[60] Zhao EM, Zhang Y, Mehl J, Park H, Lalwani MA, Toettcher JE, et al. Optogenetic regulation of engineered cellular metabolism for microbial chemical production. Nature 2018;555(7698):683–7.
[61] Zhou P, Xie W, Yao Z, Zhu Y, Ye L, Yu H. Development of a temperature-responsive yeast cell factory using engineered Gal4 as a protein switch. Biotechnol Bioeng 2018;115(5):1321–1330..
[62] Meadows AL, Hawkins KM, Tsegaye Y, Antipov E, Kim Y, Raetz L, et al. Rewriting yeast central carbon metabolism for industrial isoprenoid production. Nature 2016;537(7622):694–7.
[63] Yu W, Gao J, Zhai X, Zhou YJ. Screening neutral sites for metabolic engineering of methylotrophic yeast *Ogataea polymorpha*. Synth Syst Biotechnol 2021;6(2):63–8.
[64] Zhou YJ, Gao W, Rong Q, Jin G, Chu H, Liu W, et al. Modular pathway engineering of diterpenoid synthases and the mevalonic acid pathway for miltiradiene production. J Am Chem Soc 2012;134(6):3234–41.
[65] Reese MG. Application of a time-delay neural network to promoter annotation in the *Drosophila melanogaster* genome. Comput Chem 2001;26:51–6.